DOR: 20.1001.1.2322388.2020.8.4.1.6

Research Paper

Analytical and Numerical Evaluation of Wire Flat Rolling Process Based on the Slab Method and DEFORM-3D

Behzad Pasoodeh[1*], Hadi Tagimalek[2]

1. PhD Student, Department of Engineering, Mechanical group, Urmia University, Urmia, Iran
2. PhD Student, Faculty of Mechanical Engineering, Semnan University, Semnan, Iran

ARTICLE INFO

Article history:

Received 23 February 2020
Accepted 10 July 2020
Available online 22 October 2020

Keywords:

Wire flat rolling
Slab method
Rolling pressure
Simulation
Experimental
Symmetrical

ABSTRACT

Considering the slab method, a three-dimensional analytical model was adopted to evaluate the rolling pressure, force, and torque in symmetrical wire flat rolling. Due to the effectiveness of the shear friction model to express the frictional state in the bulk metal forming, thus, it was used to define in slab formulation. In this paper, the plains strain condition no longer is valid and, the strain on z-direction must also be taken into account in calculations. The resultant differential equations were solved numerically by the Rung Kutta method and MATLAB software. It was concluded that as the shear factor rises in the range of o.4<m<0.7, the pressure distribution (9%), rolling force (5%), and rolling torque (about 3% for theoretical and 9% for simulation) increase. Furthermore, as roll radius increases in the range of 75 mm<R<100 mm, rolling pressure (3%) and rolling force (4.4% for theoretical and 5.5% for simulation) drop while rolling torque (8% for theoretical and 4% for simulation) goes up linearly. It was found that the center of the deformed wire at the first stages of the rolling is intensively prone to crack ignition. To verify the validity of the proposed slab method, the commercial FEM software, DEFORM-3D, and other researchers' findings were applied, and an appreciative agreement was found among them, where 9% and 7% differences were obtained, respectively. Moreover, the theoretical method was compared with Kazeminezhads' experimental force, and results showed a difference below 3% at the first stages; however, as the process continues, this difference rises slightly up to18%.

Nomenclature

h_i	Initial diameter (mm)	k	Shear yield stress (MPa)
F	rolling force	φ	Contact angle (degree)
σ_x	Stress in the rolling direction (MPa)	p	Rolling pressure (MPa)
R	Roll diameter (mm)	L	Length of the deformation area (mm)
h_o	Final thickness (mm)	b	Width of the contact area (mm)
		m	Shear factor

* **Corresponding Author**:
E-mail: b.pasoodeh@urmia.ac.ir

1- Introduction

In the wire flat rolling process, the gap of two rolls welcomes the unrolled wire to obtain the desired shape in the output of the rolling zone. The initial material for the rolling process is a wire with a circular cross-section, and the resultant product is a flattened wire with a round edge on both sides of the rolled wire. The flattened wire has been applied in wide areas such as manufacturing piston rings, electrical equipment, spring wire, handsaw blades, and flat-wire electrode for gas metal arc welding (GMAW) [1]. In the symmetrical wire flat rolling, the peripheral speeds of rolls, roll diameter, and friction condition of the work rolls must be the same.

Due to the industrial applications and the great importance of controlling the manufacturing system of rolled wire, the various methods have considered the different aspects of this process. Carlsson studied the pressure distribution of the wire flat rolling process and concluded that the maximum pressure appears at the entry of the deforming area. Kazeminezhad and Karimi Taheri [2] inspected the influence of the roll speed, thickness reduction, and wire material on the width of the contact area and lateral spread of wire by the experimental method of symmetrical wire flat rolling process. They developed an expression to obtain the width of the contact area based on the wire thickness in the deforming zone. Considering microstructural evaluation on the wire rolling, Pasoodeh et al. [3] showed that, in the asymmetrical wire rolling of brass, how initial parameters influence the inhomogeneity on the rolled wire, output curvature, mechanical properties, and microstructure. The findings depicted that, as the initial microstructure be homogenous, the resultant curvature will be reduced. Moreover, they revealed that the higher roll radius ratio causes lower mean hardness on cross-section. They [4] also considered experimentally the asymmetrical wire rolling of copper. They founded that, as grains size in unrolled wire rises, the resultant curvature radius at the exit of the deformation zone as well as the width of the rolled wire is reduced. Parvizi et al. [5] studied numerically and experimentally the resultant curvature and width of the contact area in the asymmetrical wire rolling where the roll speed ratio, roll diameter ratio, and rolling height reduction was accepted as input variables. They concluded that as roll radius ratio and height reduction increase, the curvature radius decreases. Kazeminezhad and Karimi Taheri [6] examined the influence of the roll velocity and thickness reduction on rolling force and deformation condition of symmetrical wire flat rolling process. Following their previous papers, they [7] studied the inhomogeneity of deformation area in the flattened wire rolled in the symmetrical condition by applying the finite element method (FEM).

Among existing procedures analyzing rolling, the slab is the most well-known method. However, a great number of slab inspections have focused on analyzing sheet rolling. Gudur et al. [8] proposed an analytical model for the asymmetrical cold sheet rolling to evaluate the friction coefficient based on the resultant radius of the rolled sheet. They ignored the spread of the sheet in the transverse direction and assumed the constant shear stress through the thickness of the vertical side of the element in the analysis. Considering plain strain conditions, Yong et al. [9] studied the slab method for the asymmetrical rolling process. In their slab analysis, the normal stresses were assumed constant on the vertical side of the element, and the shear stresses were neglected in the evaluation. Having regarded strain hardening and Wanheim and Bay's friction model, Kumar and Dixit [10] developed the slab analysis of the foil-rolling process. Chen et al. [11] proposed a theoretical model for rolling a large cylindrical shell by slab method. They applied a mixed friction model consisting of Coulomb and sticking friction to state the interface friction state. Qwamizadeh et al. [12] developed a theoretical model with slab method to calculate the asymmetrical rolling of bonded two-layer sheets. Zhang et al. [13] developed an analytical method to evaluate the rolling force and torque in asymmetrical sheet rolling. To verify the validity of their analytical method, they conducted a comparison study of the rolling force and torque with the experimental and analytical results of other investigators. Moreover, a newly-developed-method solution for asymmetrical rolling of the unbounded clad sheet was proposed by Afrouz and Parvizi [14]. They assumed the constant shear friction model (τ= mk) as well as the non-uniformity of the stresses (shear and normal) at the slab model. Tzou and Huang [15] investigated the minimum thickness by considering the constant shear friction model (τ=mk) in the asymmetrical cold-and-hot rolling process. In addition, Tzou [16] achieved an analytical approach to study how friction factor and friction coefficient are related to the asymmetrical sheet rolling process. Iankov [17] estimated the effects of the friction and back and front tension on the contact pressure distribution and lateral spread in the symmetrical wire flat rolling process. Parvizi et al. [18] developed an analytical approach for the ring rolling process with a constant shear friction model (τ = mk). It was assumed that the normal and shear stresses through the vertical sides of the slabs are distributed nonlinearly. Hamidpour et al. [19] expanded an upper bound analysis to calculate rolling

torque in the wire rolling process. They proposed a parametric streamline and then developed an admissible velocity field. The results depicted that the wire diameter, roll speed, and reduction in height have significant influences on rolling torque.

Due to the long width of the sheet in the direction perpendicular to the rolling axis, the plane strain condition can be considered. Consequently, the lateral spread of the sheet is negligible, while this condition cannot be assumed in wire flat rolling since strains in the z-direction (perpendicular to rolling direction) must be taken into account. Thus, in addition to wire height variations, the variations of wire width must also be regarded in the slab formulation of this process. Thus, this complicated situation causes slab analysis to remain so limited in the case of wire rolling. Kazeminezhad and Karimi Taheri [20] expanded slab analysis for symmetrical rolling and evaluated the influences of the thickness reduction, coefficient of friction, and yield stress on the location of neutral points, rolling pressure, and force in the symmetrical wire flat rolling. However, they did not apply the shear friction model, where they used the Coulomb model without simulation. Based on the modified slab method, Parvizi et al. [21] studied the influences of the roll diameter ratio, friction factor ratio, and reduction in height on the force, pressure, and torque. They concluded that the rolling force and pressure could be reduced by increasing the asymmetrical nature of the process, such as a higher friction factor ratio or rolls peripheral diameter ratio.

Inspection of the literature showed that almost all proposed slab formulations had applied Coulomb friction model in their calculations. However, this form of presentation of the frictional condition usually cannot define the interfacial state accurately in the bulk metal forming processes such as rolling, forging, and extrusion. Thus, in this paper, it was motivated to propose a slab analysis based on the shear friction model, which can formulate the frictional condition between wire and rolls accurately. Moreover, due to the lack of comparative study analyzing theoretically and numerically the symmetric wire rolling, the numerical code of DEFORM 3-D was adopted to execute the simulation considerations. The numerical procedure also studied the strain distribution and crucial points to crack initiation. Moreover, to further verification of the proposed slab method, other investigators findings were applied to examine the validity of the proposed slab formulation, and, finally, the effectiveness and efficiency of the applying shear friction model in slab formulation was proven.

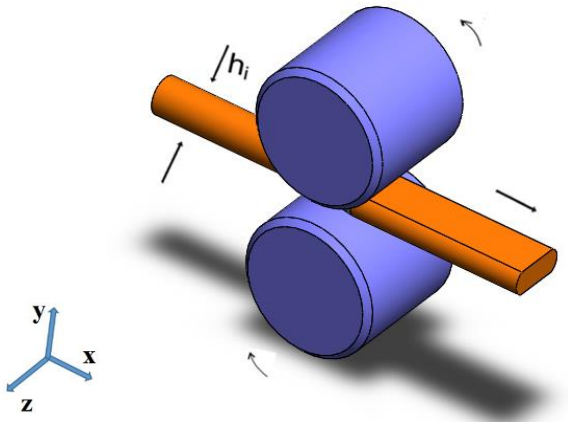

Fig. 1. Symmetrical wire rolling process. (x= Rolling direction, y= Normal direction, z= Transfer direction)

2- Mathematical model

Figure 1, shows the symmetrical wire flat rolling geometry, where there is a point which the velocity of wire becomes equal to the peripheral velocity of rolls, in which from the entry of the deformation zone until that point, the velocity of rolls exceed that of wire's, and at the remaining length the velocity of wire is more than that of rolls'. Therefore, it can be clearly mentioned that the rolling plastic deformation zone can be divided into two various zones, as shown in Figure 2. In zone I ($0 \leq x \leq x_n$), the peripheral speed of rolls is more than the speed of the wire, and the frictional stresses on the upper and the lower sides of the slab are in the forward direction. The horizontal distance from the entry plane in the rolling deformation zone in the rolling direction is considered as the x-axis, and the origin is its intersection with the axis of perpendicular to the rolls' rotating axis. In zone II ($x_n \leq x \leq L$) in which the speed of wire is more than the peripheral speed of the rolls, and the direction of the frictional stresses on the upper and lower surfaces of the slab are backward. In spite of similarities to sheet rolling, in the wire flat rolling, the assumption of plane strain condition is

necessary, and thus, the strains in the transient direction or z-axis (perpendicular to rolling direction) must be regarded in the wire flat rolling process formulations. Therefore, a three-dimensional slab (Figure 3b) was assumed, where the deformations in the z-direction have also been taken into account. The stress fields acting on differential vertical elements at the deforming zone are shown in Figure 3a. The length of the contact area in the wire flat rolling is smaller as compared with the circumferences of the rolls and can be achieved from the following equation:

$$L = \sqrt{R\,\Delta h} \quad (1)$$

The width of the contact area in the symmetrical wire flat rolling process can be obtained as follows [20]:

$$b = \sqrt{2h_i\,\Delta h} \quad (2)$$

where Δh and h_i are the reduction in height and initial diameter of wire, respectively.

By studying presented papers in the slab formulations of the symmetrical wire rolling, it was revealed that all proposed slab formulations had applied Coulomb friction model ($\tau = \mu F$) in their calculations. However, this frictional model isn't effective and applicable in bulk metal forming operations such as wire rolling, forging, and extrusion. Thus, in this survey, the shear-friction-type model was developed to express the interfacial state between rolls and wire in slab formulations. Finally, it will be compared by slab formulation extracted by Coulomb friction model [20] to its efficiency. Eq. 3 defines the shear friction model as follows:

$$\tau = mk \quad (3)$$

where m and k are a shear factor and shear yield stress, respectively, and is the shear stress acting on between rolls and wire.

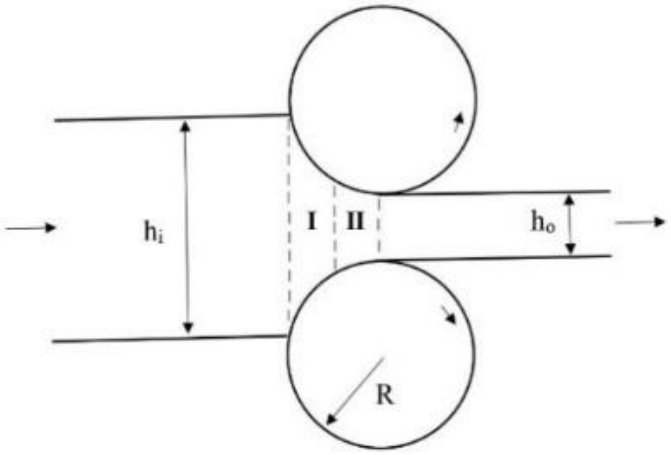

Fig. 2. Symmetrical wire flat rolling geometry.

2-1- Zone I ($0 \le x \le x_n$)

By considering horizontal and vertical equilibriums for element in zone I, following equations can be obtained, respectively.

$$[(\sigma_x + d\sigma_x)(b + db)(h + dh)] - [\sigma_x\, h\, b] + 2\left[\frac{mk\,dx\,b\sin\varphi}{\cos\varphi}\right] - 2[b\,P_I\,dx] = 0 \quad (3)$$

$$\sigma_x b\,dh + \sigma_x h\,db + h\,b\,d\sigma_x + \frac{2\,mk\,b\,x\,dx}{R} - 2\,P_I\,b\,dx = 0 \quad (4)$$

$$\sigma_y = P_I \quad (5)$$

Supposing that the shear stress in the z direction is negligible, thus, the normal stress on that direction can be considered as a principal stress. It is also assumed that the quantity of principle stress in z direction is between two other principle stresses, therefore, σ_x and σ_y become maximum and minimum stresses and finally, the Tresca yield criterion for the element on a vertical slab takes the following form:

$$\sigma_y = -P_I \quad (6)$$

$$\sigma_x + p_I = 2k \quad (7)$$

$$\sigma_x = 2k - P_I \quad (8)$$

$$d\sigma_x = -dP_I \quad (9)$$

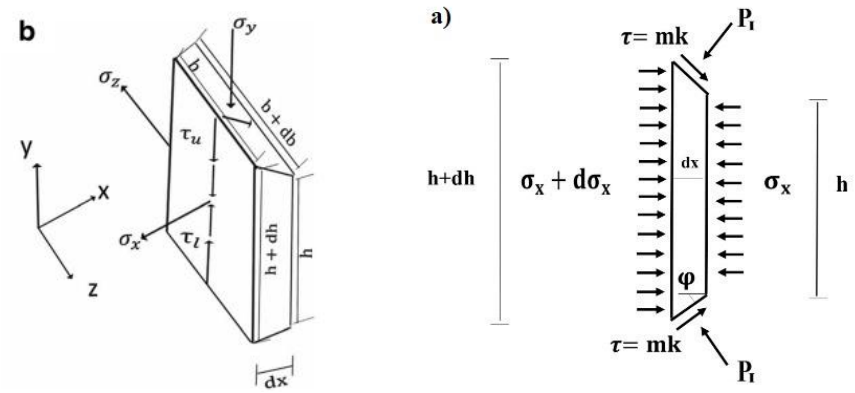

Fig. 3. (a) Stree field acting on the differential vertical element in zone I. (b) Three dimensional slab.

Regarding geometry of the element, then, the following relations can be obtained:

$$h = h_1 + \frac{x^2}{R} \quad (10)$$

$$dh = \frac{2\,x\,dx}{R} \quad (11)$$

$$b = \sqrt{4h_0\left(\frac{\Delta h}{2} - \frac{x^2}{2R}\right)} \quad (12)$$

$$db = \frac{2\,x\,h_0\,dx}{R\sqrt{4h_0\left(\frac{\Delta h}{2} - \frac{x^2}{2R}\right)}} \quad (13)$$

$$dx = R\,d\varphi \quad (14)$$

By substituting of equations (8) (9) (10) (11) (12) (13) and (14) in equation (4), below relation is given:

$$\frac{dP_I}{dx} = \frac{1}{\left(h_1+\frac{x^2}{2R}\right)}\left[(2k - P_I)\left(\sqrt{4h_0\left(\frac{\Delta h}{2} - \frac{x^2}{2R}\right)}\right)\left(\frac{2x}{R}\right)\right] + \left[(2k - P_I)\left(h_1 + \frac{x^2}{2R}\right)\left(\frac{2\,x\,h_0}{R\sqrt{4h_0\left(\frac{\Delta h}{2} - \frac{x^2}{2R}\right)}}\right)\right] + \left[\sqrt{4h_0\left(\frac{\Delta h}{2} - \frac{x^2}{2R}\right)}\ \frac{2P_I x}{R}\right] - \left[\sqrt{4h_0\left(\frac{\Delta h}{2} - \frac{x^2}{2R}\right)}\ 2\,mk\right] \quad (15)$$

Where, the initial condition of $x = 0$. $P_I = 2k$ will be selected for solving that.

2-2- II ($x_n \leq x \leq l$)

Applying the similar formulation developed in parts 2-1, the differential equation for the roll pressure in the element located in zone II is gained as follows:

$$[(\sigma_x + d\sigma_x)(b + db)(h + dh)] - [\sigma_x\,h\,b] + 2\left[\frac{mk\,b\,dx\sin\varphi}{\cos\varphi}\right] + 2[b\,P_{II}\,dx] = 0 \quad (16)$$

Final differential equation with initial condition of $x = L$, $P_{II} = 2k$ will take the following form for zone II:

$$\frac{dP_{II}}{dx} = \frac{1}{\left(h_1+\frac{x^2}{2R}\right)}\left[(2k - P_{II})\left(\sqrt{4h_0\left(\frac{\Delta h}{2} - \frac{x^2}{2R}\right)}\right)\left(\frac{2x}{R}\right)\right] + \left[(2k - P_{II})\left(h_1 + \frac{x^2}{2R}\right)\left(\frac{2\,x\,h_0}{R\sqrt{4h_0\left(\frac{\Delta h}{2} - \frac{x^2}{2R}\right)}}\right)\right] + \left[\sqrt{4h_0\left(\frac{\Delta h}{2} - \frac{x^2}{2R}\right)}\ \frac{2P_{II}x}{R}\right] + \left[\sqrt{4h_0\left(\frac{\Delta h}{2} - \frac{x^2}{2R}\right)}\ 2\,mk\right] \quad (17)$$

Finally, the resultant differential equations were solved numerically using the Rung Kutta method and MATLAB software to achieve the desired parameters.

3- Rolling Torque

By integrating the moment of shear stress about the rotating axis of rolls, aroused torque by wire on rolls can be obtained as follows:

$$T = R\left[\int_0^{x_n}(m\,k\,b)\,dx + \int_{x_n}^{l}(m\,k\,b)\,dx\right] \quad (18)$$

4- Rolling force

Considering a small contact angle of the rolls and wire, the rolling force at the interface of wire with the rolls can be achieved as follows:

$$F = \int_0^{x_n}(p_I b)\,dx + \int_{x_n}^{l}(p_{II} b)\,dx \quad (19)$$

5- Simulation procedure

The numerical evaluation was carried out to inspect the accuracy and validity of the analytical results of the wire flat rolling process for which DEFORM-3D software is used. The mesh sensitivity assessment was applied to approve the correct number of elements. To obtain the optimal size for mesh, the effect of element size on changes in equivalent plastic strain was investigated. It was observed that after the size of the 1 element, the variations of the mesh size have no effect on the strain values. Hence, this size was applied to as used element size on the current simulation. Figure (4) shows the effect of the changes in the dimensions of the element on the equivalent plastic strain variations. According to the initial dimension of unrolled wire, 55 elements in the unrolled wire cross-section with the arrangement shown in Figure 5a, were regarded.

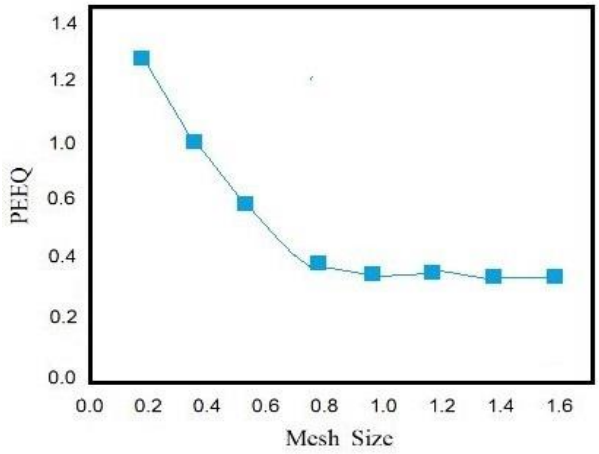

Fig. 4. Mesh Sensitivity Diagram for the equivalent plastic strain.

Table 1. Material characteristics used in this survey [21].

Material	Shear yield stress (k)	Modulus of elasticity (GPa)	Poisson's ratio	Density (kg/m3)
UNS C23000	125	115	o.31	8940

Because of the frictional condition, the deformation gap welcomes the round wire, and flattened wire is a resultant product at the exit of the deformation zone. Figure 5b shows the FEM modeling in DEFORM-3D software, and the material used in the paper is copper UNS C23000 adapted from reference [21], as given in Table 1.

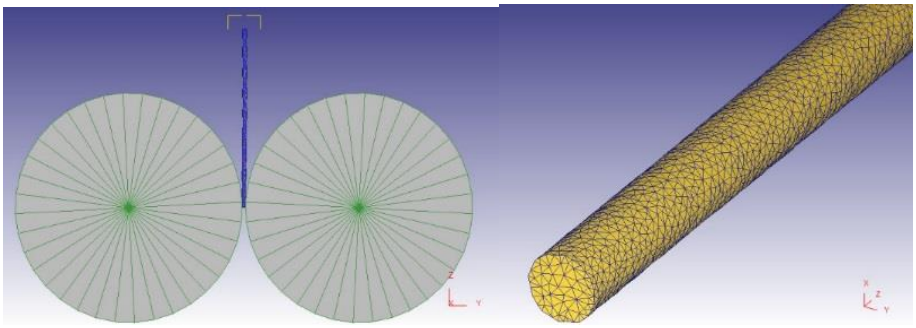

(a) (b)

Fig. 5. (a) Meshing of wire in FEM. (b) FEM modeling.

7- Results and discussions

7-1- Theoretical results and comparative outcomes

A glance at the graph provided in Figure 6 shows the effects of the shear factor on rolling pressure distribution for UNS C23000 material. The various shear factors were considered as a variable parameters to study the different conditions of the process pressure. It elucidates a point, namely the natural point (where the rotating velocity of the rolls and linear velocity of the wire are the same), meeting a maximum pressure value. However, after this point, the latter is appeared by a sharp fall for all conditions. As seen obviously, as the shear factor rises, the rolling pressure increases, where about 8% difference for two shear factors of m1 and m2 have been obtained, and the position of the natural point moves towards the exit of the deformation zone. However, the length of the contact area enjoys no changes and remains constant for all values of the shear factors. Influences of the roll radius on the rolling pressure have been shown in Figure 7 and reveal that as roll radius increases, the process pressure rises, which is mainly due to the fact that the pressure concentrates in small length for lower roll radius, but this increase isn't considerable and reaches the maximum of 3% depicting that roll changes has negligible effects on rolling pressure. Given graph depicts that there is a steep rise in pressure until the length of 4mm reaching about 300 MPa. However, it continued by a sharp downward trend lasting for just over 278 MPa in the length of 7 mm. Figure 8 reveals a comparative investigation among current study, simulation, and M. Kazeminezhad's work [20]. As can be seen, the simulation allocates the highest value due to considering all real rolling condition characteristics such as strain hardening and inhomogeneous deformation.

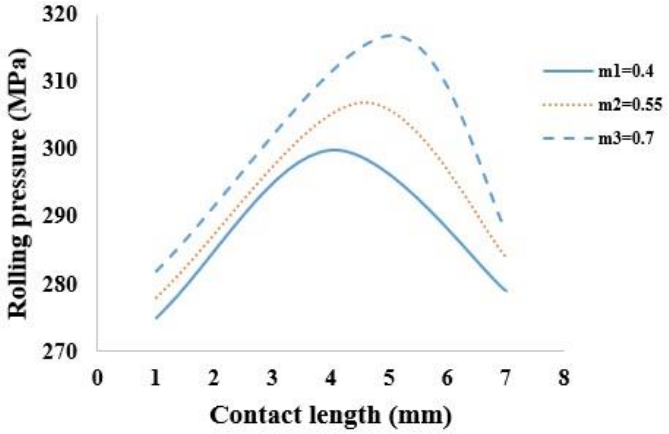

Fig. 6. Effect of the various shear factors on the rolling pressure (R=80mm, h_i= 6mm, Δh= 1.1 mm k=125 MPa.

Another crucial point to be considered is that the current theoretical slab method (developed by shear factor ratio model, $\tau = mk$) owns less values compared by kazeminezhad's one (developed by Coulomb friction model, $f = \mu N$) which seems to be due to the nature of the bulk metal forming processes (such as wire rolling). The shear factor model results in better and precision outcomes; therefore, the results that is close to the simulation method and more accurate than the Coulomb model.

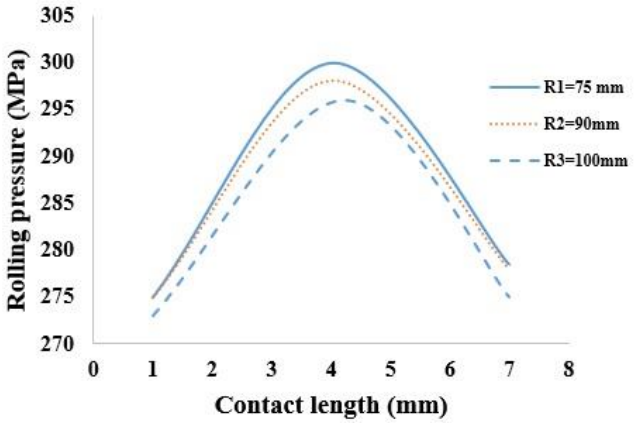

Fig. 7. Effect of the various roll radius on rolling pressure (m_1=0.4, Δh= 1.1 mm, h_i= 6mm, k=125 MPa).

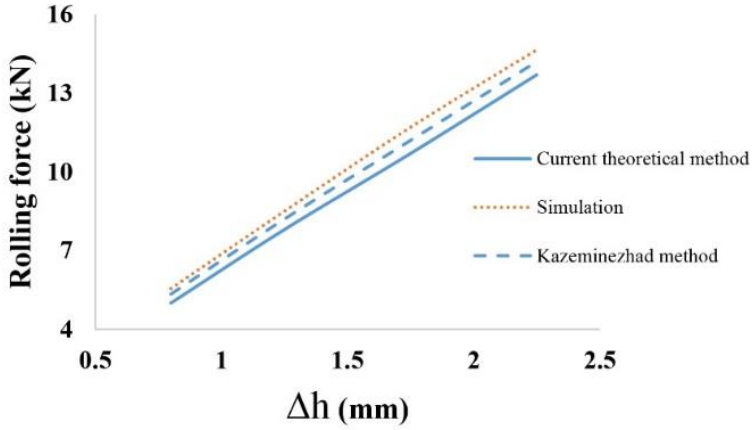

Fig. 8. Comparison study among current theoretical method, simulation and Kazeminezhd's results (Δh= 1.1 mm, R=75mm, h_i= 5.5mm, k=125 MPa).

A comparative evaluation has been made to show the effects of the variations of a shear factor on the rolling force for both simulation and theoretical procedures, as illustrated in Figure 9. It is seen that the increase of rolling force versus the shear factor for both conditions follows a linear trend on the

whole length and, in spite of the having lower values for theoretical way, still suitable agreement is appeared between them, where the maximum difference reaches 3%. Figure 10a indicates the influence of the various roll radius on the rolling force for both theoretical and simulation methods; it is noteworthy that the simulation values are bigger than theoretical ones, which can be due to the assumptions having been made for the theoretical way. As a whole, the given graph discloses a steep drop lasting until the end of the deformation zone for both methods, which is appeared more intensive for the theoretical one, and finally, they enjoy a minimum value of about 5.37 kN at the end of the deformation zone. Variations between theoretical and simulation methods are related to consumptions made in theoretical ones, such as lack of heat generation, uniformity of the applied stresses, elastic deformation, and so on. Moreover, to further validate the validity of the current theoretical method, it was compared by Kazeminezhads' experimental force (figure 10-b). It shows that, at the first stages of the process, their difference is below 3%; however, as it continues, at the final stages, their variations become over 18%. This difference is due to the ignorance of thermal effects and other simplifications made for a theoretical method, which enhance as the process goes on.

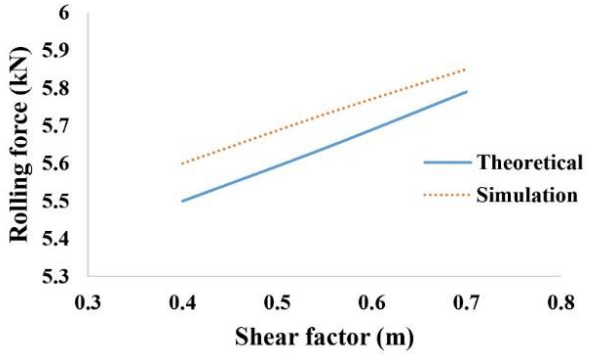

Fig. 9. Comparative study of the effect of the various shear factor on rolling force (R= 75 mm, Δh= 1.1 mm, h_i= 6mm, k=125 MPa).

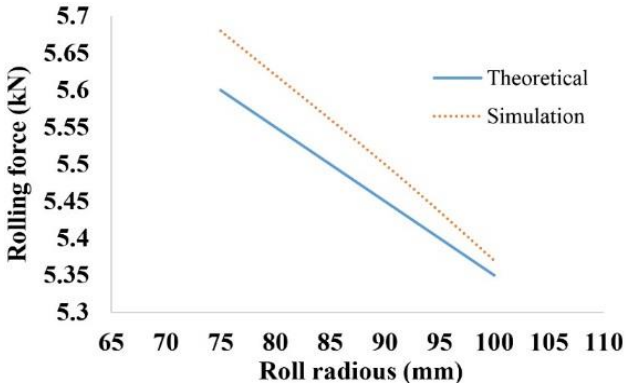

(a)

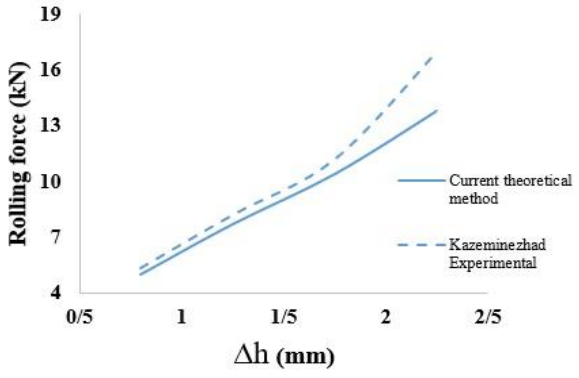

(b)

Fig. 10. A:Comparative study of the a: influence of the various roll radius on rolling force for theoretical and simulation (m- 0.4, Δh= 1.1 mm, h_i= 6mm, k=125 MPa), and b: Current theoretical method and Kazeminezhads' experimental results [20]

The effect of the shear factor on the rolling torque is demonstrated in Figure 11, where the theoretical results are compared with the simulation ones. It is seen that the values aren't in good conformity where the theoretical method leads to be horizontal, but simulation results grow steadily, and at the end of the deformation zone, their difference reaches 18%. Therefore, it is easy to understand that the assumptions made for the theoretical method affect its results and may reduce the efficiency of the study. Figure 12 illustrates the effect of the roll radius on the rolling torque for both theoretical and simulation methods. As seen, the roll radius affects rolling torque linearly in both theoretical and simulation where the slope for theoretical one is intensive compared by simulation diagram.

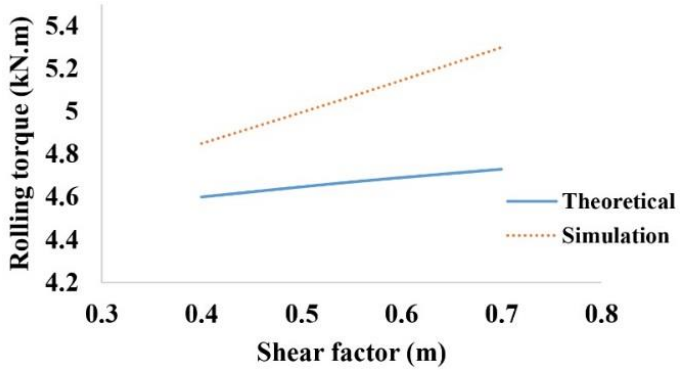

Fig. 11. Variations of shear factor versus the rolling torque for both theoretical and simulation methods (R=80 mm, Δh= 1.1 mm, h_i= 6mm, k=125 MPa)

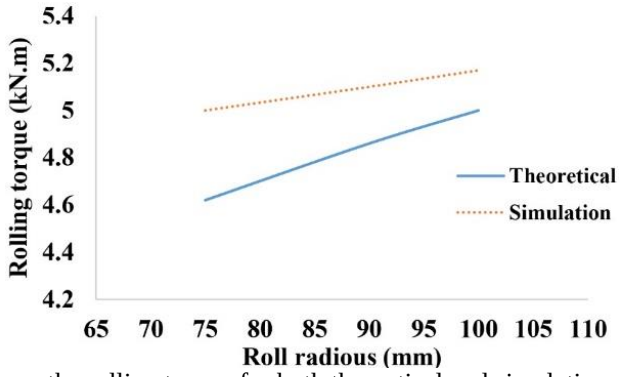

Fig. 12. Effect of the roll radius on the rolling torque for both theoretical and simulation methods (m= 0.4, Δh= 1.1 mm, h_i= 6mm, k=125 MPa).

7-2- Simulation results

As mentioned previously, in order to determine the internal deformation mechanism and variation of strain values over the wire flat rolling process, DEFORM-3D software with rigid-plastic mechanics model was applied to simulate the process, and conclusively, some results were obtained. Figures 13a, b, and c depict undeformed, partially deformed, and fully deformed of wire, respectively, and based on the calculated results from the above model, the equivalent effective strain distribution (Figure 13c) indicates that deformation of the wire rolling is very inhomogeneous throughout the rolling process, and deformation degree has a great regional difference, where, the strain of point 3 is remarkably larger than those of points 1,2 and 4 as shown in Figure 14. This phenomenon is due to the effect of external friction from the contact area with the rollers on the direction perpendicular to the rolling axis, limiting the metal flow, causing to form two upper and lower symmetrical larger cone-shaped zones on both sides. The range of the cone-shaped zone can be reduced by decreasing friction. As can be seen clearly, although, in the first steps of the rolling process, the strain of point 1 is larger than of point 2, finally, the strains of points 1 and 2 are 0.106 and 0.148, respectively demonstrating that as the rolling process runs, the influences of the frictional condition are intended, where, as being away from the center, the strain values rise meeting its peak value on the corner of the cross-section. According to the obtained results, the metal in the drum area below the corners (cone-shaped or point 4) deforms easily during rolling since the material can move freely without frictional effects. However, the equivalent strain in this area is much less than that in the center (point 3).

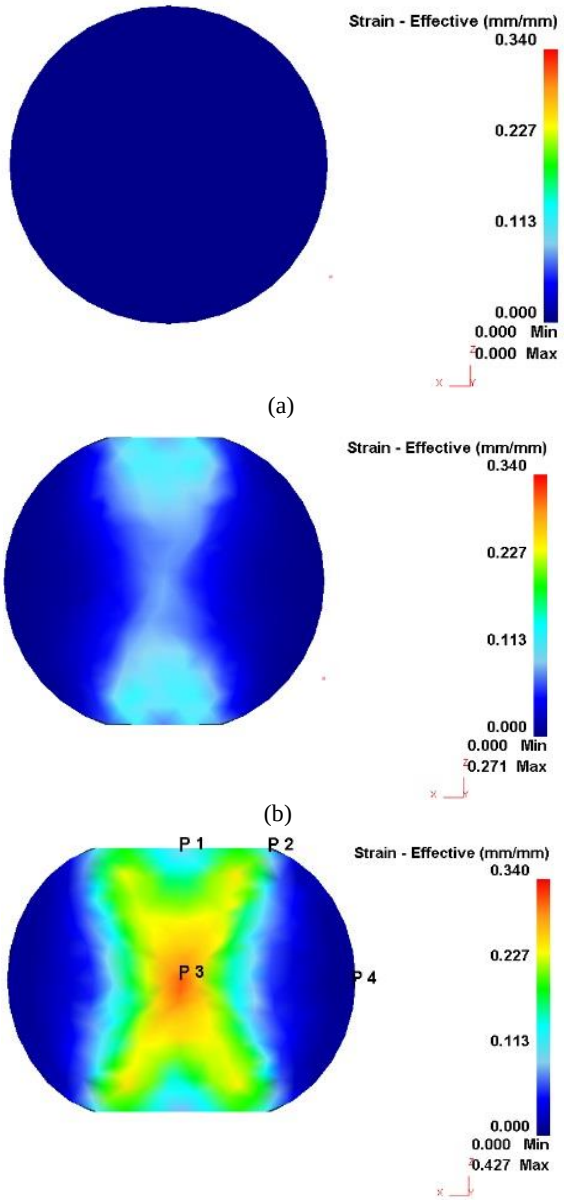

Fig. 13. Effective strain distribution for, (a): undeformed (b): partially deformed (c): fully deformed.

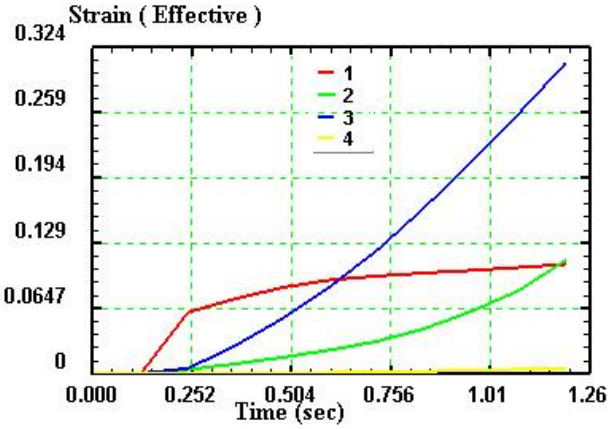

Fig. 14. Effective strain curves for points shown in Figure 13c.

Figures 15a, b, and c depict the gradient of effective strain on the sections of the rolled wire along the rolling direction (y-axis) in two various planes, including x-y and y-z planes. In spite of uniform distribution of strain on the x-y plane in the y-direction as shown in Figure 15b, in the front of the rolled wire at the center of that (along the y-direction), there is a maximum value for strain showing that once the undeformed wire enters between two rolls, the strain on the center of section is large, however, as wire moves, this strain becomes less lasting with that value until the end. Moreover, as moving towards the outer surfaces (in the direction of the x-axis), the effective strain gradient falls gradually, however after some distance from the center, the section enjoys almost zero effective strain gradient, and it is an area where the cone-shaped region has appeared. Figure 15c illustrates the gradient of effective strain on y-z plane, and it is clearly seen that, at the center of the section, the strain owns the most values. Finally, it can be concluded that the center of the deformed wire in the first steps of rolling has by far the most effective strain (as shown by the arrow in Figure 16). Therefore, this region tolerates high stress and strain over the process and subsequently is intensively prone to crack initiation.

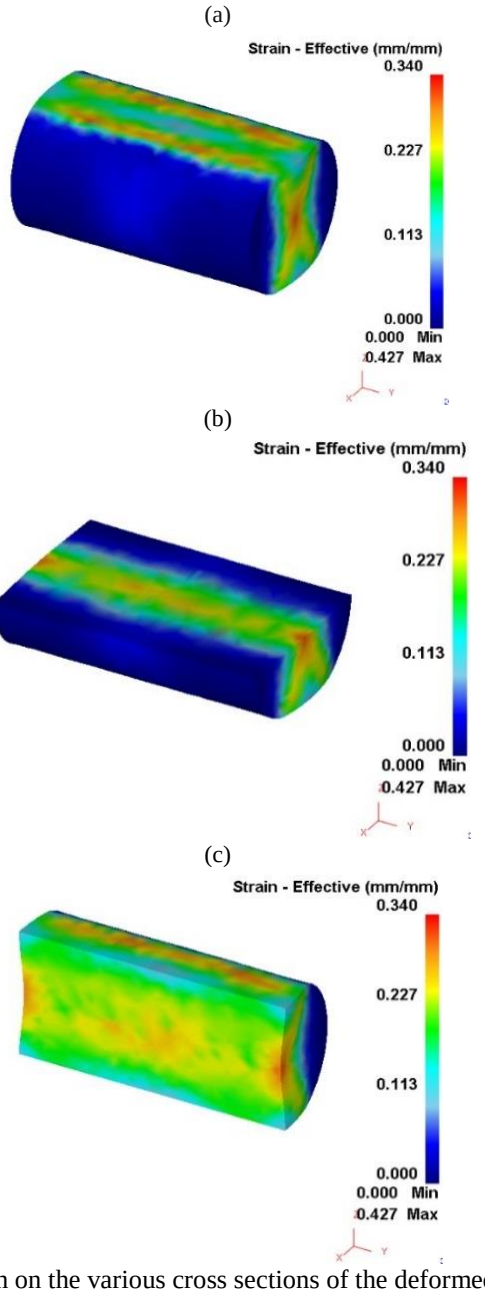

Fig. 15. Effective strain distribution on the various cross sections of the deformed wire on the rolling direction.

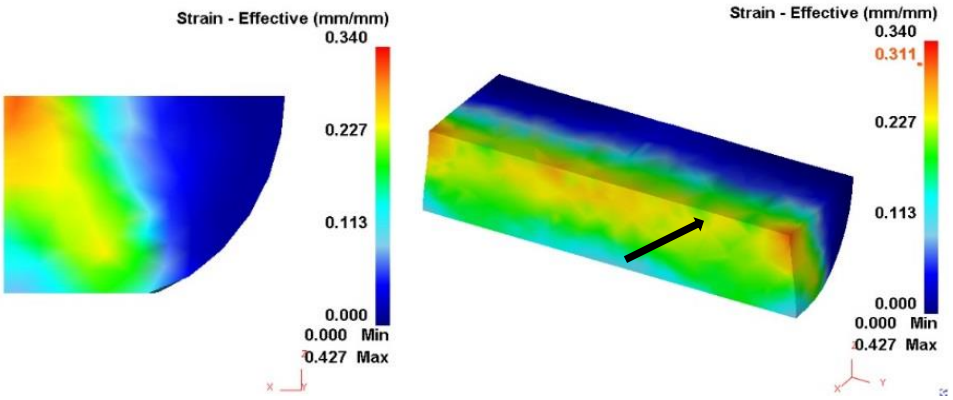

Fig. 16. Position of the crucial point for effective strain.

As it is known, having a uniform distribution of the mechanical properties along the section is of great importance, and all engineering attempts are to achieve a proper distribution, and surely, this fact works on the wire rolling processes as well. Hence, the effective strain distribution in x-direction has been achieved in diagram form showing almost linear behavior in the majority of the distance, which can help designers to evaluate appreciate calculations while predicting uniformity of the mechanical characteristics as shown in Figures 17a and b.

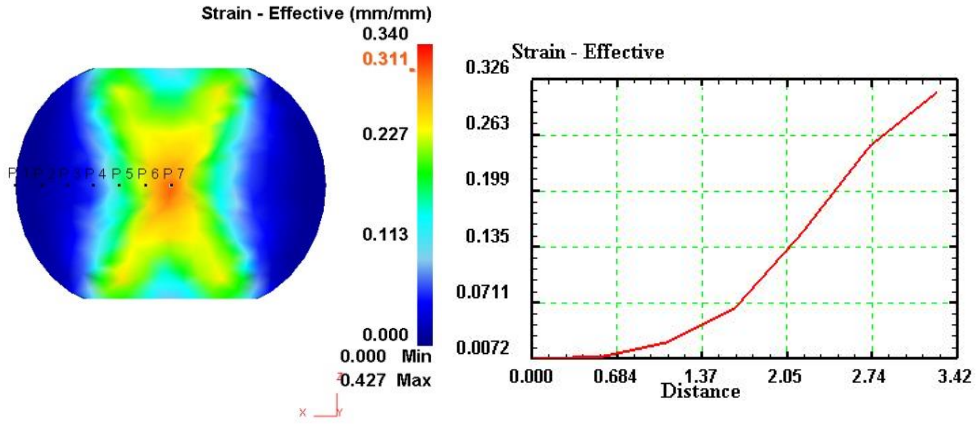

(a) **(b)**

Fig. 17. Effective strain distribution in the cross section perpendicular to rolling direction a: Contour. b: Diagram.

8- Concluding remarks

In this survey, theoretical and numerical studies were carried out. Finite element software of Deform 3-D and shear factor friction model ($\tau = \mathrm{mk}$) were applied to the numerical and slab approach, respectively, and the results were compared by Kazeminazhad's findings (slab method by Coulomb friction model) as well. Ultimately, the suitable agreement was observed between the current theoretical slab method and simulation approach, and reported important results were listed as follows:

(1) The effects of the shear factor on rolling pressure distribution were investigated, and it was found that the diagram grows rapidly until a particular point called natural point and enjoys its maximum value. However, the latter lasted with a steep decline for the rest. The maximum difference for pressures reaches 9% at natural points of diagrams.

(2) A comparative study has been conducted between the current study and Kazeminezhad and et al. [20], where there is about 10% difference between their values on whole distance. It was disclosed that when the shear factor friction model was chosen for wire rolling, the results were in better accuracy compared with the Coulomb friction model.

(3) The variations of a shear factor on the rolling force for both simulation and theoretical procedures were studied, and it was seen that the greatest difference reaches 4% at the first stages of the rolling, and as the process goes on, they tend to reduce their distance. A similar diagram was obtained for the effect of the roll radius on the wire rolling force, and it was concluded that as the roll radius rises to 100 mm, the rolling force drops to 5.38 kN and furthermore, both theoretical and simulation are going to coincidence at this point.

(4) The effect of the shear factor on the rolling torque was evaluated for both numerical and theoretical ones and seen that the highest values for shear factor (0.7) cause the greatest values for rolling torque where the slope of the simulation is a little more than a theoretical one, and finally their difference reaches to 14%. The influences of the roll radius on the rolling torque for both theoretical and simulation methods were also calculated as well. It was figured out that the variations of the roll radius affect the rolling torque noticeably. Nevertheless, the slope of the theoretical trend is steeper than simulation one, where at the entrance of the process, their difference is about 6%, and as the process goes on, this enjoys the value of 3%.

(5) To further validate the validity of the current theoretical method, it was compared by Kazeminezhads' experimental force. It is revealed that, at the first stages of the process, their difference is below 3%. However, as it continues, at the final stages, their variations become over 18%. This difference is due to the ignorance of thermal effects and other simplifications made for a theoretical method that enhances as the process goes on.

(6) The numerical results by Deform 3-D software show that, over the simulation of the symmetrical wire flat rolling process, an inhomogeneous strain distribution throughout rolled wire was seen, and deformation degree has a great regional difference where the maximum value of strain was found in the center of the rolled section with the value of 0.32 and based on the simulation predictions, that area is the most dangerous place for occurrence of the damage and strongly prone to crack initiation. Also, due to the influences of the frictional condition acting on the contact area of the wire with the rollers, cone-shaped zones on both sides appeared.

(7) The effective strain distribution in x-direction was achieved, and it was seen that there is an almost linear behavior in the majority of the distance (here radius of the rolled wire).

Reference

[1] H. Tagimalek, M. Azargoman, M.R. Maraki, M. Mahmoodi, "The effects of diffusion depth and heat-affected zone in NE-GMAW process on SUH 310S steel using an image processing method", Inter Jour of Iron & Steel Society of Iran., Vol. 17, Issue. 1, No. 1, 2020, pp. 11-20.

[2] M. Kazeminezhad, A. Karimi Taheri, "A theoretical and experimental investigation on wire flat rolling process using deformation pattern", J. Mater. Des., Vol. 26, 2008, pp. 99–103.

[3] B. Pasoodeh, A. Parvizi, H. Akbari, "Effects of asymmetrical rolling process on the micro hardness and microstructure of brass wire", JCAMECH., Vol. 49, 2018, pp. 143-148.

[4] B. Pasoodeh, A. Parvizi, H. Akbari, "Investigation of microstructure and mechanical properties in asymmetrically rolled copper wire", Journal of the Brazilian Society of Mechanical Science and Engineering., Vol. 30(30), 2017, pp. 5109-5116.

[5] A. Parvizi, B. Pasoodeh, K.Abrinia, H. Akbari, "Analysis of curvature and width of the contact area in asymmetrical rolling of wire", Journal of Manufacturing Process., Vol. 20, 2017, pp. 245-249.

[6] M. Kazeminezhad, A. Karimi Taheri, "An experimental investigation on the deformation behavior during wire flat rolling process", J. Mater. Process. Technol., Vol. 160, 2005, pp. 313-320.

[7] M. Kazeminezhad, A. Karimi Taheri, "Deformation inhomogeneity in flattened copper wire", J. Mater. Des., Vol. 28, 2007, pp. 2047-2053.

[8] PP. Gudur, M. Salunkhe, U.S. Dixit, "A theoretical study on the application of asymmetric rolling for the estimation of friction", Int. J. Mech. Sci., Vol. 50, 2008, pp. 315-327.

[9] T. Yong, G. Yan-hui, ZD. Wang, GD. Wang, "Analysis of rolling pressure in asymmetrical rolling process by slab method", J. Iron. Steel. Res. Int., Vol. 16(4), 2009, pp. 22-26.

[10] D. Kumar, U.S. Dixit, "A slab method study of strain hardening and friction effects in cold foil rolling process", J. Mater. Process. Technol., Vol. 171, 2006, pp. 331-340.

[11] S. Chen, H. Liu, Y. Peng, J. Sun, "Slab analysis of large cylindrical shell rolling considering mixed friction", Int. J. Mech. Sci. Technol., Vol. 30, 2014, pp. 4753-4760.

[12] M. Qwamizadeh, M. Kadkhodaei, M. Salimi, "Asymmetrical rolling analysis of bonded two-layer sheets and evaluation of outgoing curvature", Int. J. Adv. Manuf. Technol., Vol. 73, 2014, pp. 521-533.

[13] S.H. Zhang, D.W. Zhao, C.R. Gao, G.D. Wang, "Analysis of asymmetrical sheet rolling by slab method", Int. J. Mech. Sci., Vol. 65, 2012, pp. 168-176.

[14] F. Afrouz, A. Parvizi, "An analytical model of asymmetric rolling of unbounded clad sheets with shear effects", Journal of Manuf Process., Vol. 20, 2016, pp. 162-171.

[15] G.Y. Tzou, M.N. Hang, "Study on minimum thickness for asymmetrical hot-and-cold PV rolling of sheet considering constant shear friction", J. Mater. Process. Technol., Vol. 119(3), 2001, pp. 229-233.

[16] G.Y. Tzou, "Relationship between frictional coefficient and frictional factor in asymmetrical sheet

rolling", J. Mater. Process. Technol., Vol. 86, 1999, pp. 271-277.
[17] R, Iankov, "Finite element simulation of profile rolling wire", J. Mater. Process. Technol., Vol.142, 2003, pp. 355-361.
[18] A. Parvizi, B. Pasoodeh, K. Abrinia, H. Akbari, "Analysis of curvature and width of the contact area in asymmetrical rolling of wire", Journal of Manufacturing Processes., Vol. 20, 2015, pp. 245-249.
[19] S.P. Hamidpour, A. Parvizi, A. Seyyed Nosrati, "Upper bound analysis of wire flat rolling with experimental and FEM verification", Meccanica., Vol. 54, 2019, pp. 2247-2261.
[20] M. Kazeminezhad, A. Karimi Taheri, "Calculation of rolling pressure distribution and force in wire flat rolling process", J. Mater. Process. Technol., Vol. 171, 2006, pp. 253-258.
[21] A. Parvizi, B. Pasoodeh, K. Abrinia, "An analytical approach to asymmetrical wire rolling process with finite element verification", Int. J. Adv. Manuf. Technol., Vol. 82, 2015, pp. 1-9.